International Journal of Nanomedicine

Dovepress
open access to scientific and medical research

Open Access Full Text Article

ORIGINAL RESEARCH

Evaluating the Use of TiO_2 Nanoparticles for Toxicity Testing in Pulmonary A549 Cells

Jana Bacova[1], Petr Knotek[2], Katerina Kopecka[2], Ludek Hromadko[3], Jan Capek[1], Pavlina Nyvltova[1], Lenka Bruckova[1], Ladislava Schröterova[4], Blanka Sestakova[4], Jiri Palarcik[5], Martin Motola[3], Dana Cizkova[6], Ales Bezrouk[7], Jiri Handl[1], Zdenek Fiala[8], Emil Rudolf[4], Zuzana Bilkova[1], Jan M Macak[3,9], Tomas Rousar[1]

[1]Department of Biological and Biochemical Sciences, Faculty of Chemical Technology, University of Pardubice, Pardubice, Czech Republic; [2]Department of General and Inorganic Chemistry, Faculty of Chemical Technology, University of Pardubice, Pardubice, Czech Republic; [3]Center of Materials and Nanotechnologies, Faculty of Chemical Technology, University of Pardubice, Pardubice, Czech Republic; [4]Department of Medical Biology and Genetics, Faculty of Medicine in Hradec Kralove, Charles University, Hradec Kralove, Czech Republic; [5]Institute of Environmental and Chemical Engineering, Faculty of Chemical Technology, University of Pardubice, Pardubice, Czech Republic; [6]Department of Histology and Embryology, Faculty of Medicine in Hradec Kralove, Charles University, Hradec Kralove, Czech Republic; [7]Department of Medical Biophysics, Faculty of Medicine in Hradec Kralove, Charles University, Hradec Kralove, Czech Republic; [8]Department of Preventive Medicine, Faculty of Medicine in Hradec Kralove, Charles University, Hradec Kralove, Czech Republic; [9]Central European Institute of Technology, Brno University of Technology, Brno, Czech Republic

Correspondence: Tomas Rousar, Department of Biological and Biochemical Sciences, Faculty of Chemical Technology, University of Pardubice, Pardubice, Czech Republic, Tel +420 466 037 707, Fax +420 466 036 361, Email Tomas.Rousar@upce.cz

Purpose: Titanium dioxide nanoparticles, 25 nm in size of crystallites (TiO_2 P25), are among the most produced nanomaterials worldwide. The broad use of TiO_2 P25 in material science has implied a request to evaluate their biological effects, especially in the lungs. Hence, the pulmonary A549 cell line has been used to estimate the effects of TiO_2 P25. However, the reports have provided dissimilar results on caused toxicity. Surprisingly, the physicochemical factors influencing TiO_2 P25 action in biological models have not been evaluated in most reports. Thus, the objective of the present study is to characterize the preparation of TiO_2 P25 for biological testing in A549 cells and to evaluate their biological effects.

Methods: We determined the size and crystallinity of TiO_2 P25. We used four techniques for TiO_2 P25 dispersion. We estimated the colloid stability of TiO_2 P25 in distilled water, isotonic NaCl solution, and cell culture medium. We applied the optimal dispersion conditions for testing the biological effects of TiO_2 P25 (0–100 $\mu g.mL^{-1}$) in A549 cells using biochemical assays (dehydrogenase activity, glutathione levels) and microscopy.

Results: We found that the use of fetal bovine serum in culture medium is essential to maintain sufficient colloid stability of dispersed TiO_2 P25. Under these conditions, TiO_2 P25 were unable to induce a significant impairment of A549 cells according to the results of biochemical and microscopy evaluations. When the defined parameters for the use of TiO_2 P25 in A549 cells were met, similar results on the biological effects of TiO_2 P25 were obtained in two independent cell laboratories.

Conclusion: We optimized the experimental conditions of TiO_2 P25 preparation for toxicity testing in A549 cells. The results presented here on TiO_2 P25-induced cellular effects are reproducible. Therefore, our results can be helpful for other researchers using TiO_2 P25 as a reference material.

Keywords: titanium dioxide, nanoparticles, P25, nanotoxicity, A549 cells, dispersion

Introduction

A number of studies testing nanomaterial (NM) toxicity has been steadily increasing over past years. NMs can be used for various purposes based on their unique properties, which, in particular, are linked with their size below 100 nanometers in at least one of their dimensions.[1] However, the small size can also raise some questions on their biological effects in cells and organisms. Thus, studying biological effects of NMs, ie the estimation of their cytotoxicity or biocompatibility, is of great importance for our society.[2–5]

Received: 19 May 2022
Accepted: 21 August 2022
Published: 13 September 2022

The lungs are one of the most common entrance points of NMs into the human body.[6] Several biological models have been introduced for testing of pulmonary toxicity. The most common approach to evaluate pulmonary toxicity is represented by in vitro models including human cell lines.[7–9] One of those, the human lung adenocarcinoma epithelial A549 cell line, was initiated in 1972.[10] A549 cells contain multilamellar cytoplasmic inclusion bodies typical of those found in type II alveolar epithelial cells.[10] A549 cells have been widely used in reports estimating pulmonary toxicity of NMs, eg silica (SiO_2), iron oxides (Fe_xO_y), zinc oxide (ZnO), titanium dioxide (TiO_2),[11–13] silver (Ag)[14] nanoparticles and other specifically functionalized nanoparticles,[15] nanofibers,[16,17] nanosheets[18] and carbon-based nanomaterials.[19,20]

A variety of TiO_2 NMs, eg nanoparticles,[21] nanofibers[17] and nanotubes,[22] has been developed. All these NMs have been evaluated for biological effects because TiO_2 has been used in medicine, material science and industry. In vitro studies describing cellular effects of TiO_2 nanoparticles (NPs) have been reported most frequently, especially using the pulmonary A549 cell line.[23] Interestingly, the reports on TiO_2 NPs biological effects have provided findings of different extent of NPs-induced toxicity in A549 cells.

To date, more than 40 studies have reported results on the effects of 25 nm sized TiO_2 nanoparticles (P25) in A549 cells. Those studies have differed in dispersion techniques, tested concentration, incubation period, toxicity assay, or presence of fetal bovine serum.[24–27] The biological effect of TiO_2 P25 on proliferation and viability of A549 cells was estimated using cytotoxicity assays, including formazan-derived MTT[28]/XTT[29]/WST-1[30,31] and Trypan Blue Exclusion (TBE) tests.[24] An executive overview of these published results is provided in Table 1 that shows that the biological effect of TiO_2 P25 in A549 cells ranged from reporting negligible effects[32–36] to finding substantial cellular impairment.[11,37–40] Based on this discrepancy, we decided to estimate the factors influencing detected biological effects.

Thus, the aim of the present study was to determine the optimal conditions for testing of biological effects of TiO_2 P25 in A549 cells, including material characterization, estimation of dispersion conditions, optimization of cell culture and toxicity testing. Then, we aimed to use the optimal parameters of TiO_2 P25 preparation for biological testing in two independent cellular laboratories and to compare obtained results. An essential topicality of present study can be also supported by frequent use of TiO_2 P25 as a comparative material for evaluation of biological effects in newly developed NMs.[21,37,41,42]

Materials and Methods

Chemicals and Materials

Titanium dioxide nanoparticles (P25; anatase/rutile mixture, Product no. 718467, LOT MKCD 8503), glutaraldehyde, cacodylate buffer, osmium tetroxide, propylene oxide, lead citrate, Epon 812 and Durcupan, WST-1 reagent, monochlorobimane, formaldehyde, Triton X-100, phalloidin-FITC (phalloidin-fluorescein isothiocyanate) and fluorescence dye Hoechst 33258 were purchased from Sigma-Aldrich (USA). Uranyless was purchased from Delta Microscopies (France). Minimum Essential Medium, fetal bovine serum (FBS), pyruvate, glutamine, HEPES, penicillin, streptomycin, and

Table 1 Overview of Reports Testing TiO_2 P25 Biological Effect in A549 Cells

Detection of Cell Impairment [100 μg.mL^{-1} TiO_2 P25]	Tested Dose of TiO_2 P25 [μg.mL^{-1}]	Sonication/ Duration	Viability Test/ References
No	≤ 800	Probe/10 min	MTS[31]
No	≤ 250	Probe/16 min	WST-1[32]
No	≤ 1000	N.D.	WST-1[38]
No	≤ 100	N.D.	MTT[33]
Yes	≤ 1000	Bath/30 min	MTS[35]
Yes	≤ 100	Probe/30 min	MTT[36]
Yes	≤ 200	Bath/15 min	MTT[34]
Yes	≤ 75	Bath/15 min	MTT/WST-1[37]

Dulbecco's phosphate buffered saline (DPBS) were purchased from Invitrogen-Gibco (USA). Chloromethyl-2',7'-dichlorodihydrofluorescein diacetate (CM-H_2DCFDA) was obtained from Thermo (USA). Multi-walled carbon nanotubes (JRCNM40003a, MWCNTs) were obtained from JRC Nanomaterials Repository as a reference material.

Characterization of TiO_2 P25

The size and morphology of TiO_2 P25 were characterized by a field-emission scanning electron microscope JSM 7500F (SEM, JEOL, Japan). X-ray diffraction (XRD) analysis was carried out using Panalytical Empyrean with Cu tube and Pixcel^{3D} detector. The diffractometer was set up in Bragg–Brentano geometry. The diffractogram was taken at range 5–80 degree 2Theta. Raman scattering spectrum of TiO_2 P25, excited by a laser operating at 785 nm, was obtained using a Dimension P2 (Lambda Solution, USA).[43] The topology of TiO_2 P25 surface was monitored on an atomic force microscope Dimension Icon (Bruker, Germany) in PeakForce Quantitative Nanoscale Mechanical mode using ScanAsyst-Air tips (k = 0.4 N/m) according to the described procedure.[44]

TiO_2 P25 Dispersion Techniques

TiO_2 P25 stock solutions (10 mg.mL^{-1}) were prepared in distilled water. Different techniques were used to disperse TiO_2 P25, ie (1) manual shaking by hand in a tube, (2) sonication using ultrasonic probe UP400S, 400 W, 24 kHz (Hielscher Ultrasonics GmbH, Germany), equipped with titanium sonotrode H14 (14 mm in diameter) with the application of half of the cycle and maximal power, (3) FisherBrand FB15053H ultrasonic bath, 560 W (Fisher Scientific, UK), and (4) Ultra-turrax® disperser T10 (IKA-Werke GmbH & Co. KG, Germany) equipped with a dispersion tool (S 10 D-7 G-KS-65) at 13,000 rpm. The dispersion of 100 µg.mL^{-1} TiO_2 P25 was carried out for up to 60 min. Then, the mean hydrodynamic diameter D_H was measured by 90Plus/BI-MAS Analyzer (Brookhaven Instruments Corp., USA) using dynamic light scattering (DLS). D_H values were measured for 30 s (n = 10) and these data were statistically processed according to ISO 13321/22412.[45]

In addition, TiO_2 P25 stock solutions (10 mg.mL^{-1}) were prepared in distilled water, 0.9% NaCl and Minimum Essential Medium for cell culture w/wo 10% FBS. The stock solutions were diluted to obtain the final concentration 100 µg.mL^{-1} TiO_2 P25, vortexed for 1 min and dispersed in ultrasonic bath K2, 60 W, 33 kHz (Kraintek, Slovakia) for 10 min. Average particle size was determined by dynamic light scattering using a Zetasizer Nano ZS (Malvern Panalytical Ltd., United Kingdom). The measurements were performed at 25 °C, with a scattering angle of 173°, using disposable sizing cuvettes. Each measurement was performed in 10 repeats after 30 s. Data were statistically processed.

Endotoxin Contamination

TiO_2 P25 were suspended in endotoxin-free water and diluted at 1 mg.mL^{-1} concentration. Nanoparticles were vigorously vortexed, sonicated for 15 min and centrifuged (15,000*g*; 15 min). The endotoxin concentration was measured in the supernatant using the PyroGene™ Recombinant Factor C Assay (Lonza, Blackley, UK). According to manufacturer´s instructions, the presence of endotoxin in a sample was calculated using the standard curve and results were expressed as endotoxin concentration in EU.mL^{-1}.

Cell Culture

The A549 cell line was purchased from the American Type Culture Collection (ATCC, Manassas, VA, USA). The cells were cultured in Minimum Essential Medium with 10% (v/v) FBS, 2 mmol.L^{-1} glutamine, 1 mmol.L^{-1} pyruvate, 10 mmol.L^{-1} HEPES, 50 µmol.L^{-1} penicillin/streptomycin and maintained at 37 °C in a sterile humidified atmosphere of 5% CO_2. TiO_2 P25 treatment was initiated at 70% of confluence. The cells were proven to be Mycoplasma-free and the origin of the cells was confirmed by STR analysis.

Cell Treatment with TiO_2 P25

For in vitro experiments, stock solutions of 10 mg.mL^{-1} TiO_2 P25 and MWCNTs were dispersed in culture medium w/wo FBS. Then, the stock solutions were vortexed for 1 min and sonicated for 10 min using ultrasonic bath K2. The working

solutions were prepared by dilution in the culture medium without phenol red to obtain final concentrations of 1, 10, and 100 $\mu g.mL^{-1}$.

A549 cells were seeded into 96-well plates at density of 10×10^3 cells per well. After 24 h of seeding, the cells were exposed to 1, 10, and 100 $\mu g.mL^{-1}$ TiO_2 P25. The cells were incubated with TiO_2 P25 at 37 °C in 5% CO_2 for 24 h. Unexposed cells were used as a negative control and MWCNTs were used as a positive control.

For inter-laboratory comparison of TiO_2 P25-induced biological effects in A549 cells, the described above conditions for TiO_2 P25 preparation were used. Two independent laboratories, namely, Laboratory I (Department of Biological and Biochemical Sciences, Faculty of Chemical Technology, University of Pardubice, Czech Republic) and Laboratory II (Department of Medical Biology and Genetics, Charles University, Faculty of Medicine in Hradec Kralove, Czech Republic) prepared TiO_2 P25 stock solutions independently (10 $mg.mL^{-1}$ TiO_2 P25 in cell culture medium with 10% FBS; sonication for 10 min using ultrasonic bath). Then, the working solutions were prepared by their dilution in the culture medium to obtain the final concentration 1–100 $\mu g.mL^{-1}$. A549 cells were seeded into 96-well plates at density of 10×10^3 cells per well for 24 h. Then, the cells were treated with TiO_2 P25 for 24 h and biological effect was tested using the WST-1 test.

Dehydrogenase Activity Measurement

The cell viability was assessed using the WST-1 test. The WST-1 test measures the activity of mitochondrial dehydrogenases.[46] After incubation with nanomaterials, 10 µL of WST-1 reagent was added to each well containing cells in 100 µL of culture medium according to the manufacturer's instructions. After 1 h, the change of absorbance was measured at the wavelength of 440 nm using SPARK microplate reader (Tecan, Austria) or at 450 nm with 650 nm reference wavelength using SPEKTRAFluor Plus (Tecan, Austria) while incubated at 37 °C. The dehydrogenase activity was expressed as the percentage of total cellular dehydrogenases activity relative to that in control cells (control = 100%).

Measurement of Glutathione Levels

The glutathione (GSH) levels were measured using an optimized monochlorobimane assay.[47] The working solution of monochlorobimane (MCB) was prepared fresh at the time of analysis by dilution in Dulbecco's phosphate buffer and tempered at 37 °C. After the treatment, 20 µL of the MCB solution was added to the cells in 96-well plates and the measurement started immediately. The final concentration of MCB in a well was 40 $\mu mol.L^{-1}$. The fluorescence intensity (Ex/Em = 394/490 nm) was measured kinetically for 20 min using SPARK microplate reader (Tecan, Austria). The fluorescence was expressed as the slope of a fluorescence change over time. GSH levels were expressed as the percentage relative to GSH levels in control cells (control = 100%).

Transmission Electron Microscopy

A549 cells were fixed in 3% glutaraldehyde (in 0.1 $mol.L^{-1}$ cacodylate buffer, pH 7.2) after quick and gentle wash in 0.1 $mol.L^{-1}$ cacodylate buffer (pH 7.2) directly in the culture flask, for 5 min at 37 °C and then for 3 h at room temperature. Following rinsing in 0.1 $mol.L^{-1}$ cacodylate buffer (pH 7.2), the cells were post-fixed in 1% osmium tetroxide (in 0.1 $mol.L^{-1}$ cacodylate buffer, pH 7.2) for 1 h at room temperature, washed in cacodylate buffer (0.1 $mol.L^{-1}$, pH 7.2) and dehydrated in graded alcohols (50%, 75%, 96% and 100%). For clarification, propylene oxide was used and subsequently, the cells were embedded in the mixture of Epon 812 and Durcupan (polymerization for 3 days at 60 °C). Ultrathin sections cut on Ultrotome Nova (LKB, Broma, Sweden) were collected onto formvar carbon-coated copper grids (Plano, Wetzlar, Germany) and counterstained with uranyl acetate using Uranyless and lead citrate. In a JEOL JEM-1400Plus transmission electron microscope (TEM, at 120 kV; JEOL, Japan) the ultra-thin sections were observed, and images were captured with the integrated 8Mpix CCD camera and using software TEM Center (ver. 1.7.1537; JEOL).

Detection of Nuclear Condensation and Fragmentation

To measure nuclear condensation and fragmentation in intact cells, we used a fluorescence dye: Hoechst 33258 (H33258).[48] After treatment with tested nanomaterials for 24 h, the cells grown in a 96-well plate were centrifuged (5 min; 8,000*g*; RT). Then, 70 µL of a supernatant was replaced with 70 µL of phosphate-buffered saline and 10 µL of H33258 solution was added to a well. The final concentrations of H33258 in a well was 2 $\mu g.mL^{-1}$. Then, the cells were incubated with H33258 for 5 min

and spectrofluorometric measurement was performed at Ex/Em = 352/461 nm using SPARK microplate reader (Tecan, Austria) while incubated at 37 °C. The samples were measured at least in triplicates. After background subtraction, the fluorescence signal was presented in Relative Fluorescence Units (RFU) as mean ± SEM.

Detection of Reactive Oxygen Species (ROS)

Chloromethyl-2',7'-dichlorodihydrofluorescein diacetate (CM-H_2DCFDA) was used as an intracellular probe to detect ROS production. The working solution was prepared fresh at the time of analysis by dilution in culture medium. After 24 h incubation with TiO_2 P25 and MWCNTs, 67.5 µL of CM-H_2DCFDA was added to cells to be loaded for 90 min. The final concentration of CM-H_2DCFDA in a well was 5 µmol.L^{-1}. Then, the cells were washed with phosphate buffered saline and the fluorescence (Ex/Em = 485/535 nm) was measured for 60 min using SPARK microplate reader (Tecan, Austria). The ROS levels were expressed as the percentage relative to ROS levels in control cells (= 100%).

Fluorescence Microscopy

To stain actin filaments, we used a phalloidin-FITC dye. A549 cells were seeded at density of 10×10^3 cells/well of a chamber slide. After 24 h, the cells were exposed to 1, 10 and 100 µg.mL^{-1} TiO_2 P25 or 100 µg.mL^{-1} MWCNTs. After the treatment, the A549 cells were fixed by 3.7% formaldehyde (5 min; 37 °C; dark) and permeabilized by 0.1% Triton X-100 (15 min; 37 °C; dark). Then, 100 µL of phalloidin-FITC (1 µmol.L^{-1}) was incubated for 40 min at 37 °C. After dye loading, the cells were washed two times with phosphate-buffered saline. The actin filaments (FITC filter, 480/30 nm) and morphology of A549 cells using phase contrast were observed with a fluorescence microscope Eclipse 80i (Nikon, Japan).

Data Evaluation and Statistical Analysis

All experiments were repeated at least three times independently. Three replicates were used in each independent experiment. In addition, we evaluated the interference of tested nanomaterials with the assays. We found no significant interference with most of the used assays when the background was below 10% of that in negative controls. Only in nuclear condensation and fragmentation H33258 assay, did a larger extent of interference occur in 100 µg.mL^{-1} TiO_2 P25 and 100 µg.mL^{-1} MWCNTs treated cells. The results are expressed as mean ± SD. The analysis of variance followed by Bonferroni post-test was used to perform the mean comparison at significance level $p = 0.05$.

Results

Characterization of TiO_2 P25

Firstly, we characterized shape and size of commercially available TiO_2 P25 nanoparticles (TiO_2 P25) using scanning electron microscopy. We found that TiO_2 P25 were supplied in a form of agglomerates with an average size over 1 µm in maximal dimension (Figure 1A). Those agglomerates were composed of primary particles with size 30±10 nm (Figure 1B) but the primary particles were obviously interconnected by solid bridges to each other.

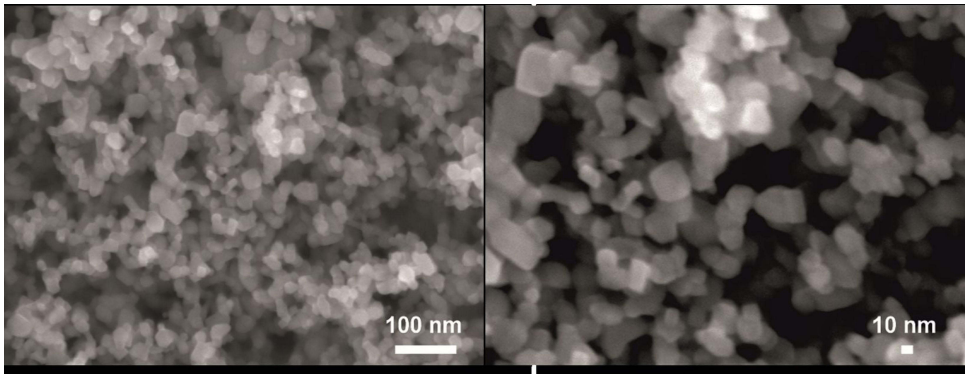

Figure 1 SEM images of TiO_2 P25 nanoparticles at two different magnifications.

The phase composition of TiO_2 P25 was analyzed by X-ray diffraction analysis (Figure 2). The sample of TiO_2 P25 consisted of 90.4% (wt) of anatase (ICDD:00–021-1272) and 9.6% (wt) of rutile (ICDD:00–021-1276) phases. The crystallite size for anatase phase of ≈ 27 nm was determined by Rietveld method. These results are in in accordance with manufacturer´s information.

Dispersion of TiO_2 P25

A proper dispersion of TiO_2 P25, ie a separation of aggregates into ideally a mixture of well-separated single particles, is a crucial point for assessment of their biological effects. Thus, the rate of dispersion of TiO_2 P25 in distilled water was tested using four techniques. Out of these, three techniques were chosen according to the most frequently used procedures in the literature, namely: hand shaking, ultrasonication in a bath and by an arc probe. In addition, we used Ultra-turrax instrument ensuring TiO_2 P25 dispersion using the maximal shear forces. In addition to the hydrodynamic diameter measurement of TiO_2 P25 dispersed for 40 min (Figure 3A), we tested the effect on duration of dispersion (Figure 3B). Our results showed that the maximal rate of dispersion of TiO_2 P25 in distilled water was found in nanoparticles dispersed using ultrasonic probe and bath. After the dispersion using ultrasonic probe, we detected a fraction of TiO_2 P25 sized under 100 nm (Figure 3A). In TiO_2 P25 dispersed using ultrasonic bath, the smallest fraction of nanoparticles was about 150 nm in size. The use of both techniques, however, provided also fractions of

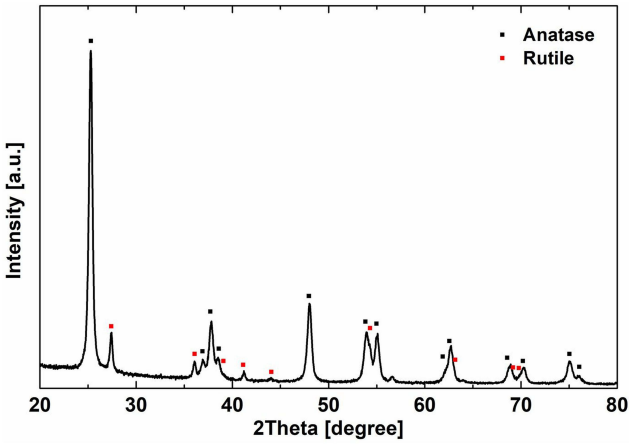

Figure 2 XRD patterns of TiO_2 P25 nanoparticles showing anatase (black) and rutile (red) peaks. The sample of TiO_2 P25 consisted of 90.4% (wt) of anatase (ICDD:00–021-1272) and 9.6% (wt) of rutile (ICDD:00–021-1276) phases.

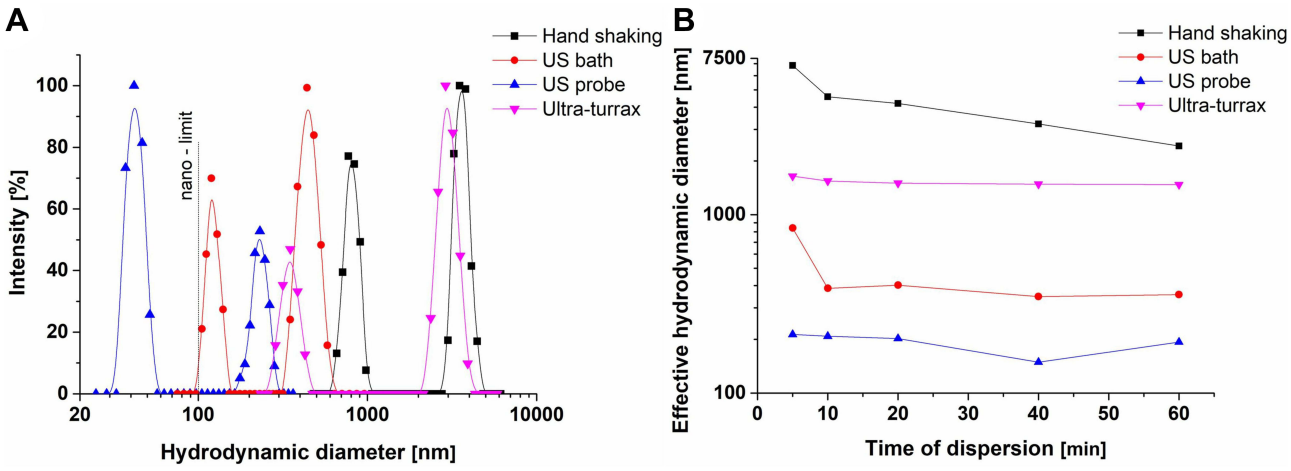

Figure 3 Results of dispersion of TiO_2 P25 in distilled water (100 $\mu g.mL^{-1}$) using four dispersion techniques: hand shaking, ultrasonic (= US) bath, US probe and Ultra-turrax. The particle size distribution was measured - (**A**) directly after finished 40 min dispersion, or (**B**) after various dispersion times between 5–60 min.

dispersed nanoparticles being larger than 200 nm (Figure 3A). The use of Ultra-turrax and hand shaking caused dispersion of TiO_2 P25 at limited extent only. Our results on the extent of TiO_2 P25 dispersion in time (Figure 3B) showed that the effective hydrodynamic diameter remained predominantly stable. The duration to obtain the maximal rate of dispersion was determined to be at least 10 min.

The results from the testing of different dispersion techniques were obtained in TiO_2 P25 diluted in distilled water. Generally, the testing of NMs in cells, however, requires a use of culture media containing all necessary ingredients to ensure the cell growth and proliferation. Thus, we tested the behavior of TiO_2 P25 in distilled water in comparison to the dispersion stability in saline solution and Minimum Essential cell culture medium with or without addition of 10% fetal bovine serum. Our previous results showed that the dispersion of TiO_2 P25 using ultrasonic probe or ultrasonic bath provided comparable results on dispersion of nanoparticles in complex matrix of cell culture medium. Thus, we used the dispersion of TiO_2 P25 nanoparticles using ultrasonic bath for 10 min following the procedure described below.

We determined the relation of obtained extent of TiO_2 P25 dispersion and used environment (Figure 4). As expected, the dispersion of TiO_2 P25 in distilled water provided a small fraction of TiO_2 P25 about 150 nm in size but the large population of nanoparticles aggregates remained over 400 nm in size. No dispersed TiO_2 P25 aggregates under 400 nm in size were detected in NaCl solution and in culture medium without FBS. On the other hand, the presence of FBS in cell culture medium stabilized the dispersion of nanoparticles providing the size of TiO_2 P25 aggregates at about 100 nm in 10% of nanoparticles. The final evaluation of our data on dispersion of TiO_2 P25 provided essential information on necessity of FBS presence in assessment of biological effects of TiO_2 P25 in cell culture media to ensure as large as possible dispersion. We conclude that a number of factors have been influencing the accomplishment of proper TiO_2 P25 dispersion, ie dispersion technique, duration, ingredients in the cell culture medium and also the interval between preparation of TiO_2 P25 suspension and addition to cultured cells. Thus, in all following experiments, we prepared TiO_2 P25 suspensions using sonication in ultrasonic bath (10 min) in cell culture medium with FBS ensuring the colloidal stability.

Effect of FBS in TiO_2 P25 Treatment of A549 Cells

According to the frequent use of A549 cells in the literature,[12,28,49,50] we used this cellular model for testing of TiO_2 P25 biological effects too. Firstly, we tested TiO_2 P25 for potential endotoxin contamination. We found that the concentration of endotoxin in the sample occurred under the detection limit of the assay (<0.005 EU.mL^{-1}). Thus, tested TiO_2 P25 were proven to be endotoxin-free.

Then, we estimated the influence of the fetal bovine serum presence on TiO_2 P25-induced biological effects. A549 cells were treated with 0–100 μg.mL^{-1} TiO_2 P25 w/wo FBS. After 24 h, we estimated an effect of TiO_2 P25 on the cell viability

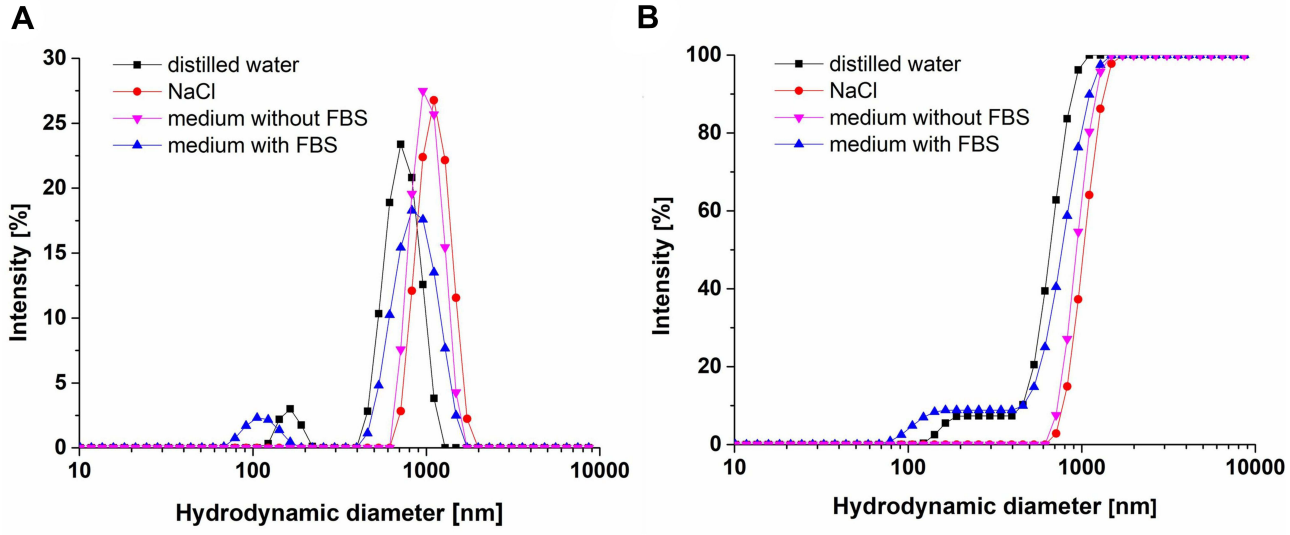

Figure 4 Results of TiO_2 P25 size distribution (100 μg.mL^{-1}) in different solutions: distilled water, 0.9% NaCl, cell culture medium w/wo 10% fetal bovine serum (FBS) for 10 min using ultrasonic bath. Data are presented as intensity distribution (**A**) and cumulative intensity (**B**) of TiO_2 P25 size.

Table 2 TiO_2 P25 Cytotoxicity Evaluation in A549 Cells. Dehydrogenase Activity (= Cell Viability, WST-1 Test) and Glutathione Levels Were Assayed in A549 Cells Treated with 0–100 $\mu g.mL^{-1}$ TiO_2 P25 in Culture Medium w/wo Fetal Bovine Serum (FBS) for 24 h. The Results are Expressed as Mean ± SD ($p < 0.001$, Compared to Untreated Cells; Three Independent Experiments)

Cell Culture	TiO_2 P25 [$\mu g.mL^{-1}$]	Dehydrogenase Activity	Glutathione Level
Without FBS	0	100 ± 3%	100 ± 3%
	1	99 ± 5%	100 ± 5%
	10	101 ± 4%	98 ± 5%
	100	97 ± 4%	85 ± 7% ($p < 0.001$)
With FBS	0	100 ± 3%	100 ± 4%
	1	97 ± 5%	104 ± 6%
	10	98 ± 8%	91 ± 4% ($p < 0.001$)
	100	97 ± 9%	87 ± 4% ($p < 0.001$)

and glutathione levels measured using the WST-1 test and monochlorobimane, respectively. The results are presented in Table 2. In A549 cells incubated with or without FBS, we found that none of the tested TiO_2 P25 concentrations affected cellular dehydrogenase activity significantly in comparison to untreated cells. A slight decrease of dehydrogenase activity to 97 ± 4% was detected only in 100 $\mu g.mL^{-1}$ TiO_2 P25 treated A549 cells with FBS. Measurement of glutathione levels, as an essential intracellular antioxidant, detected a significant glutathione depletion in 100 $\mu g.mL^{-1}$ TiO_2 P25 treated A549 cells grown both with and without FBS. The results are presented in Table 2. In addition, mild, but significant glutathione depletion was observed in A549 cells with FBS exposed to 10 $\mu g.mL^{-1}$ TiO_2 P25.

Transmission electron microscopic analyses were carried out to evaluate the effect of 10% FBS on TiO_2 P25 cellular acting. TEM photomicrographs (Figure 5) showed internalization of TiO_2 P25 (100 $\mu g.mL^{-1}$) after 24 h of incubation of A549 cells both in presence and absence of FBS. TiO_2 P25 occurred in the cytoplasm predominantly in simple or double-membrane vesicles. Near the cell surface, many slender cytoplasmic projections were formed and TiO_2 P25 were accumulated in their vicinity. The most obvious difference between A549 cells incubated with TiO_2 P25 w/wo FBS was that the nanoparticles dispersed in FBS-free medium aggregated and accumulated more around the cells (Figure 5A) comparing the cells incubated in FBS containing medium (Figure 5B). In accordance with presented results, we concluded that presence of FBS in cell culture medium ensures proper TiO_2 P25 dispersion necessary for valuable estimation of TiO_2 P25 effect in cells. Thus, we used TiO_2 P25 treatment of A549 cells in presence of 10% FBS in all following experiments.

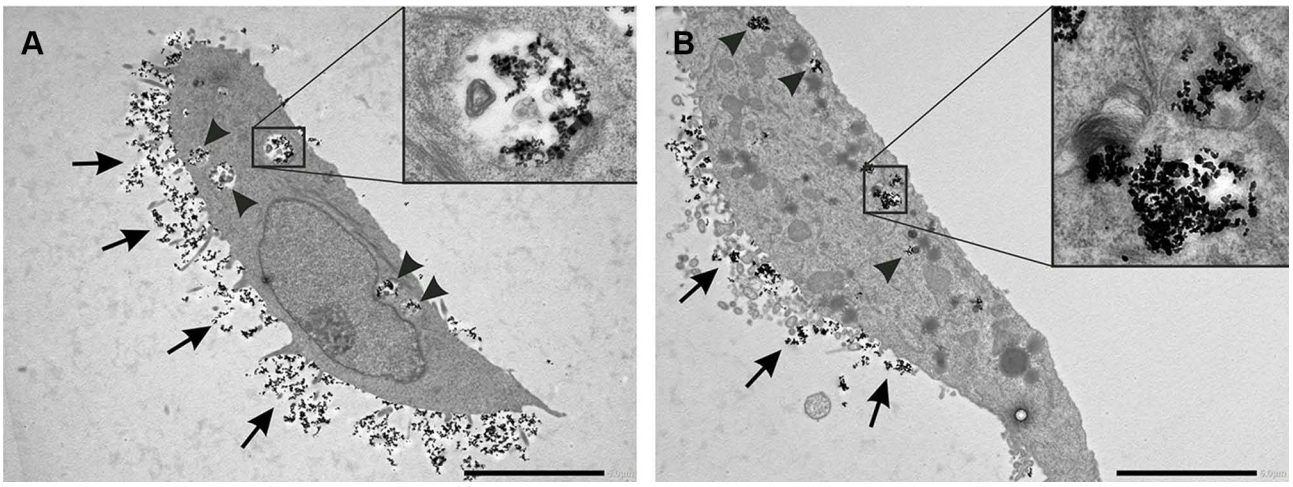

Figure 5 TEM images of A549 cells treated with TiO_2 P25 w/wo fetal bovine serum. (**A**), without FBS; (**B**), with FBS. The pictures confirmed internalization of TiO_2 P25 in the cytoplasm in vesicles (arrowheads, inserts). TiO_2 P25 accumulated in the vicinity of slender cytoplasmic projections (arrows). Scale bar = 5 μm (mag. 2500x); insert (**A**) (mag. 11,100x); insert (**B**) (mag. 14,500x).

Estimation of TiO_2 P25 Effect in A549 Cells

In addition to WST-1 and glutathione tests, we used three additional methods for characterizing the TiO_2 P25 effects in A549 cells in more detail, ie determination of nuclear condensation and fragmentation, ROS production and assessment of cell morphology. To evaluate the cellular effect, we tested TiO_2 P25 (0–100 $\mu g.mL^{-1}$) in comparison to MWCNTs (100 $\mu g.mL^{-1}$) used as a positive control (Figure 6A). After 24 h, we found that none of tested TiO_2 P25 concentrations induced significant nuclear condensation and fragmentation in comparison to untreated cells. Only a mild increase of DNA condensation was found with 100 $\mu g.mL^{-1}$ TiO_2 P25, implying that TiO_2 P25 treatment did not cause an induction of apoptotic cell death. On the other hand, a significant increase of nuclear condensation and fragmentation was detected in MWCNTs treated A549 cells.

To observe any induction of an oxidative stress after TiO_2 P25 treatment in A549 cells, we investigated the production of reactive oxygen species using a spectrofluorometric probe detecting entire ROS production. After 24 h of incubation, we did not observe any significant induction of ROS production in tested TiO_2 P25 in comparison to untreated A549 cells (Figure 6B). MWCNTs treatment, however, induced significant increase of ROS production.

Fluorescence staining of actin filaments and phase contrast microscopy were used for a visual evaluation of TiO_2 P25-treated A549 cells (Figure 6C). Typical epithelial morphology was found in both untreated and TiO_2 P25-treated A549 cells, showing no significant effect of TiO_2 P25 treatment. On the other hand, incubation of A549 cells with MWCNTs caused changes found in photomicrographs, lowering the number of cells and changing their morphology. Finally,

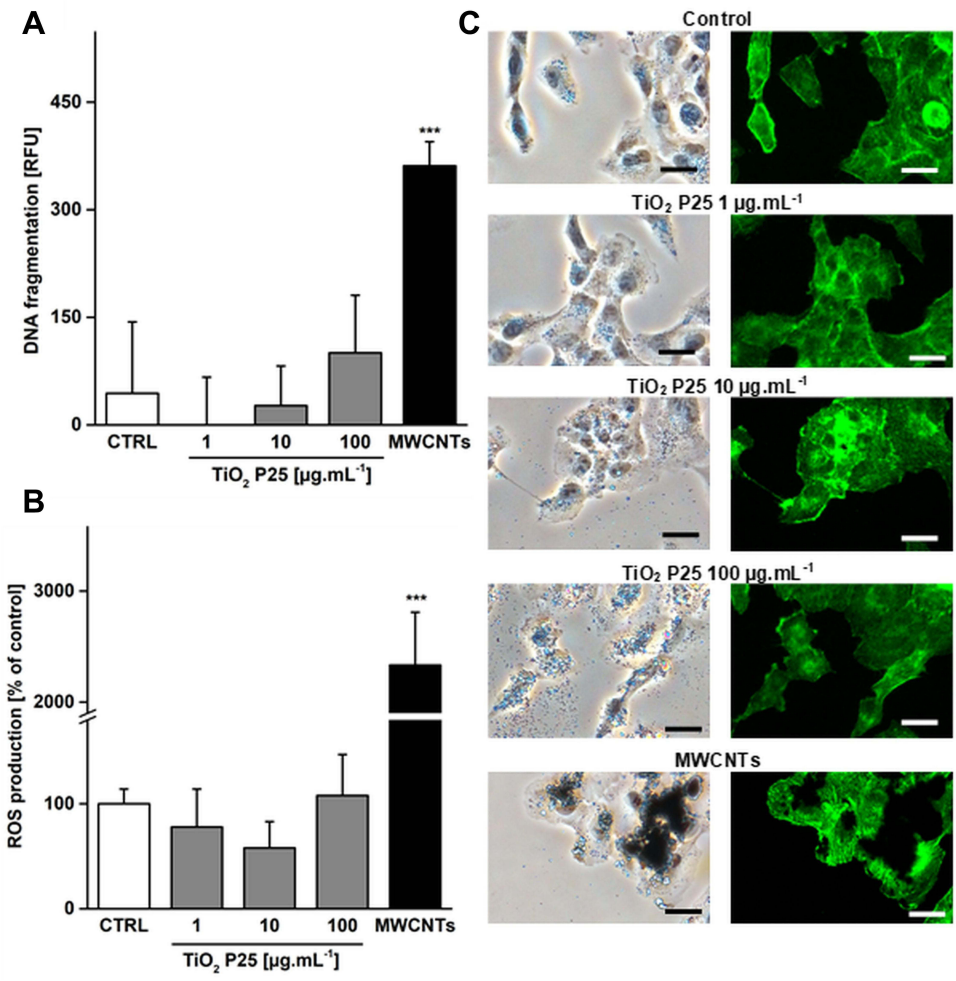

Figure 6 Estimation of TiO_2 P25 effects in A549 cells. A549 cells were treated with TiO_2 P25 (0–100 $\mu g.mL^{-1}$) and MWCNTs (100 $\mu g.mL^{-1}$) with FBS for 24 h. (**A**) nuclear condensation and fragmentation, (**B**) ROS production and (**C**) A549 cells morphology (scale bar = 10 μm) were estimated. The results are expressed as mean ± SD (***$p < 0.001$, compared to untreated cells).

Table 3 Interlaboratory Comparison of TiO_2 P25 Biological Effects in A549 Cells. A549 Cells Were Treated with TiO_2 P25 (0–100 $\mu g.mL^{-1}$) for 4 and 24 h in Two Cellular Laboratories Independently. Dehydrogenase Activity (= Cell Viability, WST-1 Test) Was Measured After Treatment. The Results are Expressed as Mean ± SD (Compared to Untreated Cells = 100%)

Time	TiO_2 P25 [$\mu g.mL^{-1}$]	Laboratory I	Laboratory II
4 h	**0**	100 ± 7%	100 ± 6%
	1	100 ± 8%	101 ± 5%
	10	100 ± 7%	98 ± 6%
	100	103 ± 7%	102 ± 5%
24 h	**0**	100 ± 5%	100 ± 6%
	1	97 ± 6%	100 ± 4%
	10	102 ± 6%	99 ± 6%
	100	96 ± 6%	99 ± 6%

according to the outcomes of all experiments using different methods for characterizing the effect of TiO_2 P25 in A549, we conclude that TiO_2 P25 treatment induced no significant cell impairment.

Interlaboratory Comparison of Biological Effects of TiO_2 P25 in A549 Cells

Finally, we aimed to estimate the reproducibility of obtained results from testing of biological effects of TiO_2 P25. Thus, the preparation, dispersion, cell treatment and evaluation of TiO_2 P25 biological effects in A549 cells was performed independently in two cellular laboratories. In Table 3, the biological effect of TiO_2 P25 (0–100 $\mu g.mL^{-1}$) was assessed using the WST-1 test in A549 cells after 4 and 24 h exposure in culture medium with FBS. In accordance with the outcomes presented above, the results from two laboratories showed that none of the TiO_2 P25 concentrations induced a significant decrease in cell viability in any of the tested time intervals. In conclusion, the results demonstrated the reproducibility of pre-analytical and analytical procedures established in the present study. In addition, our outcomes showed that TiO_2 P25 at levels up to 100 $\mu g.mL^{-1}$ do not induce any significant dehydrogenase activity decrease.

Discussion

In the present study, we aimed to evaluate the pre-analytical, analytical and biological factors having an effect on obtained outcomes from TiO_2 P25 testing in pulmonary A549 cells. In Table 1, a number of reports published very different outcomes from their experiments on testing of biological effects of TiO_2-based nanoparticles. Thus, we focused on characterization of the experimental conditions and identification of the optimal parameters for TiO_2 P25 biological assessment in A549 cells. Just as a reminder, P25 are commercially available nanoparticles, but their origin and producers have diversified over the past 20 years. We chose them because they have been used frequently in a number of reports focusing on cellular testing, especially in A549 cells.[32,51–53] In addition to TiO_2 P25, other TiO_2-based nanoparticles have also been used in scientific studies, eg Aeroxide TiO_2 P25 (Evonik, Germany),[11] TiO_2 (Sigma-Aldrich, USA),[54] TiO_2 Degussa (Korea)[55] and NM105 TiO_2 from the Nanomaterial Library at the JRC (Italy).[49] In general, the physicochemical properties of TiO_2 nanoparticles, for example size,[38] shape,[24] crystallinity form,[31] solubility, aggregation[26,56] and nanoparticle–protein interaction,[57] can affect their toxicity significantly. Nowadays, the conditions for testing and evaluating nanoparticle toxicity results differ in many parameters. Therefore, further research is important to find reliable methods for the prediction, characterization and behavior of nanoparticles in test systems.[58,59]

We characterized the shape and size of TiO_2 P25 using SEM (Figure 1). TiO_2 P25 were supplied in a form of agglomerates, which were composed of primary particles with size 30±10 nm, with an average size over 1 μm in maximal dimension. Another study showed that TiO_2 P25 (Sigma-Aldrich, USA) agglomerates, with size 378±50 nm and these NPs, were not further separable by sonication.[52] TiO_2 P25 (Sigma-Aldrich, USA) in another study exhibited an average primary size of 12–50 nm and formation of agglomerates as well.[51] This is in agreement with another published

report[60] in TiO_2 P25 NPs (Degussa, Germany), implying that used nanoparticles not 25 nm in size strongly influence their physical-chemical and biological properties.

The proper dispersion of inorganic nanoparticles in hydrophilic environment is an additional crucial point to gain valid and repeatable results in biological testing of TiO_2 P25. Although several different dispersion techniques have been used in TiO_2 P25, there is no report that would compare them – until this study. Inconsistent application of ultrasonic-based techniques across laboratories, including ultrasonic bath[38,40] or probes,[34,35] variability in experimental conditions (power, duration of ultrasonic pulse, shape of the probe, etc.), together with the duration of ultrasonication can lead to significant variability in suspension characteristics.[56] Different dispersion conditions of TiO_2 P25 stock solutions at various concentrations in water[33,54,61] or culture media[62] were described in a number of studies summarized in Table 1. We used different techniques to disperse TiO_2 P25, manual shaking by hand, ultrasonic probe, ultrasonic bath and Ultra-turrax® disperser to prepare the suspensions in distilled water. We found that FBS presence and the use of any of the ultrasonic techniques for at least 10 min led to sufficient dispersion with required stability of the TiO_2 P25 colloid. Our results on beneficial effect of FBS presence for proper dispersion can be supported by a study describing differences between TiO_2 nanoparticles sonicated in culture media with 10% FBS.[38] The effect of FBS on nanoparticle aggregation was also investigated in other studies using microscopic techniques.[26,63]

In addition, TEM analyses confirmed the advantageous effect of FBS use in A549 cells treated with TiO_2 P25. Our TEM images showed that TiO_2 P25 prepared in serum-free medium aggregated and accumulated around the A549 cells and part of TiO_2 P25 was taken up by A549 cells. This is in good agreement with previous studies.[29,32] In addition, it is important to note that testing the biological effects of nanoparticles in cell culture medium containing FBS is essential to mimic the physicochemical properties similar to human body fluids containing albumin, globulins and other plasmatic proteins acting as detergents.

In assessment of biological effects of TiO_2 P25 in A549 cells, pre-analytical factors can also influence obtained results. Not only the presence/absence of FBS during cell treatment, but also the variability in cell seeding can play an important role. For cytotoxicity testing, the number of A549 cells seeded in 96-well microtiter plates ranged from 7,500,[35] 40,000[41] to 150,000[40] cells per well. In present study, we used the density of 10,000 cells per well according to our preliminary estimation of cell confluence and viability for use in the experiments lasting for up to 48 h.

The use of specific and sensitive bioanalytical assay for characterization of nanoparticle acting in cells is also the crucial point for proper evaluation of changes in cellular status. Routine, high-throughput formazan-based methods (eg MTT, MTS, XTT, WST) detecting the changes in spectral properties after reduction have been used most frequently, as presented in Table 1. The differences in their experimental protocols and principles of detection could be the reason for differing results in published papers testing metabolic activity of cells treated with nanoparticles.[29,62] Indeed, there are also reported findings on interferences during testing of cellular effects of TiO_2 nanoparticles in the case of MTT[62,64] and neutral red assay.[62] Furthermore, Ag NPs and Fe_2O_3 showed interferences with MTT, MTS, WST-8 assays.[65] Despite those reports, former but also recent papers have not taken into account the interference of nanoparticles with used assays.[66] An additional reason for different outcomes from scientific studies testing NPs could be different experimental protocols because some authors described that, after treatment, they washed the cells before toxicity evaluation using dehydrogenases assays.[35,62] This procedural approach, however, could lead to loss of some cells together with NPs.

Based on a thorough review of the literature, we decided to use the WST-1 test and to evaluate the dehydrogenase activity changes in cells. After treatment of A549 cells with TiO_2 P25, we did not find any significant difference in cellular dehydrogenases activity after 24 h. Our results agree with the outcomes of other studies. After 24 h, no cytotoxicity was observed in TiO_2 P25 up to 2,160 $\mu g.mL^{-1}$ measured by MTT test.[32] Another study found no impairment in A549 cells treated with TiO_2 NPs (Aeroxide P25, Evonik, USA) up to 1,000 $\mu g.mL^{-1}$ using the MTS assay.[26] Any significant effect of TiO_2-based nanoparticles on A549 cell viability was not found in the case of other studies testing concentrations in the range 0–200 $\mu g.mL^{-1}$.[67,68]

Because glutathione, an essential intracellular antioxidant, can act against increased ROS production, we expected finding of glutathione depletion in A549 cells treated with TiO_2 P25. Indeed, after 24 h, we found significant glutathione depletion in 100 $\mu g.mL^{-1}$ TiO_2 P25 treated cells. Also other reports published results on glutathione depletion caused by TiO_2 nanoparticles treatment in A549 with 10 or 250 $\mu g.mL^{-1}$ after 4 or 24 h, respectively.[36,69]

Furthermore, we assessed nuclear condensation and ROS production in A549 cells. Our results showed that none of the TiO_2 P25 concentrations induced significant nuclear condensation compared to untreated A549 cells after 24 h. It is obvious that TiO_2 P25 are not capable of inducing apoptosis with its typical manifestations including nuclear fragmentation. On the other hand, significant DNA damage of A549 cells detected by the comet assay was observed after the incubation with TiO_2 based nanoparticles at concentrations of 75 and 100 $\mu g.mL^{-1}$ after 6 h[70] and at 50–200 $\mu g.mL^{-1}$ after 48 h.[71] These findings, however, can also be associated with nuclear processes other than apoptosis.

In addition, ROS production estimated using ROS-probes was found to be only insignificantly increased after 100 $\mu g.mL^{-1}$ TiO_2 P25 treatments for 24 h. Although other reports presented findings on increased ROS production in A549 cells, the reports used different types of TiO_2 nanoparticles, implying that the different surface of NPs could lead to an increase in ROS production.[68,70] Throughout our study, we used MWCNTs as a positive benchmark material for comparison of findings in TiO_2 P25-treated A549 cells, ie in assessment of nuclear condensation and ROS production in A549 cells. MWCNTs have been used as a reference positive control in a number of recent studies.[16,17,72] We found that the treatment with 100 $\mu g.mL^{-1}$ MWCNTs induced nuclear condensation and fragmentation of DNA in A549 cells after 24 h, which is in agreement with a study describing induction of cytotoxicity and genotoxicity after cell treatment with 5–100 $\mu g.mL^{-1}$ MWCNTs for 4–24 h.[73] In addition, our finding suggesting induction of oxidative stress after 100 $\mu g.mL^{-1}$ MWCNTs treatment in A549 cells can be supported by outcomes of other studies reporting an increase of ROS production after treatment with 1–50 $\mu g.mL^{-1}$ MWCNTs for 6–24 h[74] and 100 $\mu g.mL^{-1}$ MWCNTs for short incubation time. Our results presented here on use of MWCNTs in A549 cells, therefore, show outcomes similar to other studies using MWCNTs.

Conclusion

Herein, we presented a complex study on the use of TiO_2 P25 for treatment in A549 cells. Firstly, we characterized and optimized the dispersion of TiO_2 P25 to ensure the proper stability of the nanoparticle suspension. Secondly, we estimated the biological effects in A549 showing that TiO_2 P25 did not cause any significant cell impairment expect for induction of a mild glutathione depletion at 100 $\mu g.mL^{-1}$ TiO_2 P25. This finding that TiO_2 P25, in contrast to MWCNTs, are not capable of inducing significant cell damage was supported by additional biochemical assays. Finally, we showed that our results are repeatable and can be reproduced in two laboratories independently. Because no other comparable report describing optimization and validation of TiO_2 P25 use has been published yet, we conclude that the results provided here can be very beneficial for other researchers using TiO_2 P25 as a benchmark material in the estimation of pulmonary toxicity in A549 cells.

Acknowledgments

The authors acknowledge financial support from the Ministry of Education, Youth and Sports of the Czech Republic (MEYES CR) through project NANOBIO CZ.02.1.01/0.0/0.0/17_048/0007421. SEM and XRD analyses were carried out with the support of CEMNAT Research Infrastructure (LM 2018103, MEYS CR, 2020-2022).

Author Contributions

All authors made a significant contribution to the work reported, whether that is in the conception, study design, execution, acquisition of data, analysis and interpretation, or in all these areas; took part in drafting, revising or critically reviewing the article; gave final approval of the version to be published; have agreed on the journal to which the article has been submitted; and agree to be accountable for all aspects of the work.

Disclosure

Dr Ales Bezrouk reports grants from Charles University, Faculty of Medicine in Hradec Kralove, during the conduct of the study; grants from Charles University, Faculty of Medicine in Hradec Kralove, outside the submitted work. The authors reports no other conflicts of interest in this work.

References

1. Gleiter H. Nanostructured materials: basic concepts and microstructure. *Acta Materialia*. 2000;48(1):1–29. doi:10.1016/S1359-6454(99)00285-2
2. Bhattacharya K, Kilic G, Costa PM, Fadeel B. Cytotoxicity screening and cytokine profiling of nineteen nanomaterials enables hazard ranking and grouping based on inflammogenic potential. *Nanotoxicology*. 2017;11(6):809–826. doi:10.1080/17435390.2017.1363309
3. Suttiponparnit K, Jiang J, Sahu M, Suvachittanont S, Charinpanitkul T, Biswas P. Role of surface area, primary particle size, and crystal phase on titanium dioxide nanoparticle dispersion properties. *Nanoscale Res Lett*. 2011;6(1):27. doi:10.1007/s11671-010-9772-1
4. Lewinski N, Colvin V, Drezek R. Cytotoxicity of nanoparticles. *Small*. 2008;4(1):26–49. doi:10.1002/smll.200700595
5. Geloen A, Mussabek G, Kharin A, Serdiuk T, Alekseev SA, Lysenko V. Impact of carbon fluoroxide nanoparticles on cell proliferation. *Nanomaterials*. 2021;11(12):3168. doi:10.3390/nano11123168
6. Hiemstra PS, Grootaers G, van der Does AM, Krul CAM, Kooter IM. Human lung epithelial cell cultures for analysis of inhaled toxicants: lessons learned and future directions. *Toxicol In Vitro*. 2018;47:137–146. doi:10.1016/j.tiv.2017.11.005
7. Frohlich E. Comparison of conventional and advanced in vitro models in the toxicity testing of nanoparticles. *Artif Cells Nanomed Biotechnol*. 2018;46(sup2):1091–1107. doi:10.1080/21691401.2018.1479709
8. Yoo K-C, Yoon C-H, Kwon D, et al. Titanium dioxide induces apoptotic cell death through reactive oxygen species-mediated Fas upregulation and Bax activation. *Int J Nanomedicine*. 2012;7:1203. doi:10.2147/IJN.S28647
9. Al-Rashed S, Baker A, Ahmad SS, et al. Vincamine, a safe natural alkaloid, represents a novel anticancer agent. *Bioorg Chem*. 2021;107:104626. doi:10.1016/j.bioorg.2021.104626
10. Lieber M, Todaro G, Smith B, Szakal A, Nelson-Rees W. A continuous tumor-cell line from a human lung carcinoma with properties of type II alveolar epithelial cells. *Int J Cancer*. 1976;17(1):62–70. doi:10.1002/ijc.2910170110
11. Guadagnini R, Moreau K, Hussain S, Marano F, Boland S. Toxicity evaluation of engineered nanoparticles for medical applications using pulmonary epithelial cells. *Nanotoxicology*. 2015;9(sup1):25–32. doi:10.3109/17435390.2013.855830
12. Wu B, Wu J, Liu S, et al. Combined effects of graphene oxide and zinc oxide nanoparticle on human A549 cells: bioavailability, toxicity and mechanisms. *Environ Sci*. 2019;6(2):635–645.
13. Chairuangkitti P, Lawanprasert S, Roytrakul S, et al. Silver nanoparticles induce toxicity in A549 cells via ROS-dependent and ROS-independent pathways. *Toxicol In Vitro*. 2013;27(1):330–338. doi:10.1016/j.tiv.2012.08.021
14. Baker A, Iram S, Syed A, et al. Fruit derived potentially bioactive bioengineered silver nanoparticles. *Int J Nanomedicine*. 2021;16:7711. doi:10.2147/IJN.S330763
15. Gómez-Morales J, Fernández-Penas R, Romero-Castillo I, et al. Crystallization, luminescence and cytocompatibility of hexagonal calcium doped terbium phosphate hydrate nanoparticles. *Nanomaterials*. 2021;11(2):322. doi:10.3390/nano11020322
16. Bianchi MG, Campagnolo L, Allegri M, et al. Length-dependent toxicity of TiO2 nanofibers: mitigation via shortening. *Nanotoxicology*. 2020;14(4):433–452. doi:10.1080/17435390.2019.1687775
17. Allegri M, Bianchi MG, Chiu M, et al. Shape-related toxicity of titanium dioxide nanofibres. *PLoS One*. 2016;11(3):e0151365. doi:10.1371/journal.pone.0151365
18. Tabish TA, Pranjol MZI, Hayat H, et al. In vitro toxic effects of reduced graphene oxide nanosheets on lung cancer cells. *Nanotechnology*. 2017;28(50):504001. doi:10.1088/1361-6528/aa95a8
19. Zhang D, Zhang L, Zheng W, et al. Investigating biological effects of multidimensional carboxylated carbon-based nanomaterials on human lung A549 cells revealed via non-targeted metabolomics approach. *Nanotechnology*. 2021;32(1):015704. doi:10.1088/1361-6528/abb55b
20. Di Ianni E, Moller P, Vogel UB, Jacobsen NR. Pro-inflammatory response and genotoxicity caused by clay and graphene nanomaterials in A549 and THP-1 cells. *Mutat Res Genet Toxicol Environ Mutagen*. 2021;872:503405. doi:10.1016/j.mrgentox.2021.503405
21. Thirunavukkarasu GK, Bacova J, Monfort O, et al. Critical comparison of aerogel TiO2 and P25 nanopowders: cytotoxic properties, photocatalytic activity and photoinduced antimicrobial/antibiofilm performance. *Appl Surf Sci*. 2021;579:152145.
22. Michalkova H, Skubalova Z, Sopha H, et al. Complex cytotoxicity mechanism of bundles formed from self-organised 1-D anodic TiO2 nanotubes layers. *J Hazard Mater*. 2020;388:122054. doi:10.1016/j.jhazmat.2020.122054
23. Martin A, Sarkar A. Overview on biological implications of metal oxide nanoparticle exposure to human alveolar A549 cell line. *Nanotoxicology*. 2017;11(6):713–724. doi:10.1080/17435390.2017.1366574
24. Kose O, Tomatis M, Leclerc L, et al. Impact of the physicochemical features of TiO2 nanoparticles on their in vitro toxicity. *Chem Res Toxicol*. 2020;33(9):2324–2337. doi:10.1021/acs.chemrestox.0c00106
25. Prasad RY, Wallace K, Daniel KM, et al. Effect of treatment media on the agglomeration of titanium dioxide nanoparticles: impact on genotoxicity, cellular interaction, and cell cycle. *ACS nano*. 2013;7(3):1929–1942. doi:10.1021/nn302280n
26. Tedja R, Lim M, Amal R, Marquis C. Effects of serum adsorption on cellular uptake profile and consequent impact of titanium dioxide nanoparticles on human lung cell lines. *ACS nano*. 2012;6(5):4083–4093. doi:10.1021/nn3004845
27. Vranic S, Gosens I, Jacobsen NR, et al. Impact of serum as a dispersion agent for in vitro and in vivo toxicological assessments of TiO 2 nanoparticles. *Arch Toxicol*. 2017;91(1):353–363. doi:10.1007/s00204-016-1673-3
28. Brandão F, Fernández-Bertólez N, Rosário F, et al. Genotoxicity of TiO2 nanoparticles in four different human cell lines (A549, HEPG2, A172 and SH-SY5Y). *Nanomaterials*. 2020;10(3):412. doi:10.3390/nano10030412
29. Simon-Deckers A, Gouget B, Mayne-L'Hermite M, Herlin-Boime N, Reynaud C, Carriere M. In vitro investigation of oxide nanoparticle and carbon nanotube toxicity and intracellular accumulation in A549 human pneumocytes. *Toxicology*. 2008;253(1–3):137–146. doi:10.1016/j.tox.2008.09.007
30. Kuku G, Culha M. Investigating the origins of toxic response in TiO(2) nanoparticle-treated cells. *Nanomaterials*. 2017;7(4):83. doi:10.3390/nano7040083
31. Fresegna AM, Ursini CL, Ciervo A, et al. Assessment of the influence of crystalline form on cyto-genotoxic and inflammatory effects induced by TiO2 nanoparticles on human bronchial and alveolar cells. *Nanomaterials*. 2021;11(1):253. doi:10.3390/nano11010253
32. Jayaram DT, Kumar A, Kippner LE, et al. TiO 2 nanoparticles generate superoxide and alter gene expression in human lung cells. *RSC Adv*. 2019;9(43):25039–25047. doi:10.1039/C9RA04037D

33. Hansjosten I, Rapp J, Reiner L, et al. Microscopy-based high-throughput assays enable multi-parametric analysis to assess adverse effects of nanomaterials in various cell lines. *Arch Toxicol*. 2018;92(2):633–649. doi:10.1007/s00204-017-2106-7
34. Hanot-Roy M, Tubeuf E, Guilbert A, et al. Oxidative stress pathways involved in cytotoxicity and genotoxicity of titanium dioxide (TiO2) nanoparticles on cells constitutive of alveolo-capillary barrier in vitro. *Toxicol In Vitro*. 2016;33:125–135. doi:10.1016/j.tiv.2016.01.013
35. Remzova M, Zouzelka R, Brzicova T, et al. Toxicity of TiO2, ZnO, and SiO2 nanoparticles in human lung cells: safe-by-design development of construction materials. *Nanomaterials*. 2019;9(7):968. doi:10.3390/nano9070968
36. Monteiller C, Tran L, MacNee W, et al. The pro-inflammatory effects of low-toxicity low-solubility particles, nanoparticles and fine particles, on epithelial cells in vitro: the role of surface area. *Occup Environ Med*. 2007;64(9):609–615. doi:10.1136/oem.2005.024802
37. Ahmad J, Siddiqui M, Akhtar M, et al. Copper doping enhanced the oxidative stress–mediated cytotoxicity of TiO2 nanoparticles in A549 cells. *Hum Exp Toxicol*. 2018;37(5):496–507. doi:10.1177/0960327117714040
38. Tedja R, Marquis C, Lim M, Amal R. Biological impacts of TiO 2 on human lung cell lines A549 and H1299: particle size distribution effects. *J Nanoparticle Res*. 2011;13(9):3801–3813. doi:10.1007/s11051-011-0302-6
39. Jugan M-L, Barillet S, Simon-Deckers A, et al. Titanium dioxide nanoparticles exhibit genotoxicity and impair DNA repair activity in A549 cells. *Nanotoxicology*. 2012;6(5):501–513. doi:10.3109/17435390.2011.587903
40. Rosario F, Bessa MJ, Brandao F, et al. Unravelling the potential cytotoxic effects of metal oxide nanoparticles and metal(loid) mixtures on a549 human cell line. *Nanomaterials*. 2020;10(3):447. doi:10.3390/nano10030447
41. Hsiao IL, Huang YJ. Effects of various physicochemical characteristics on the toxicities of ZnO and TiO nanoparticles toward human lung epithelial cells. *Sci Total Environ*. 2011;409(7):1219–1228. doi:10.1016/j.scitotenv.2010.12.033
42. Gea M, Bonetta S, Iannarelli L, et al. Shape-engineered titanium dioxide nanoparticles (TiO2-NPs): cytotoxicity and genotoxicity in bronchial epithelial cells. *Food Chem Toxicol*. 2019;127:89–100. doi:10.1016/j.fct.2019.02.043
43. Knotek P, Navesnik J, Cernohorsky T, Kincl M, Vlcek M, Tichy L. Ablation of (GeS2) 0.3 (Sb2S3) 0.7 glass with an ultra-violet nano-second laser. *Mater Res Bull*. 2015;64:42–50. doi:10.1016/j.materresbull.2014.12.027
44. Kopecká K, Melánová K, Beneš L, Knotek P, Mazur M, Zima V. Exfoliation of layered mixed zirconium 4-sulfophenylphosphonate phenylphosphonates. *Dalton Trans*. 2020;49(12):3816–3823. doi:10.1039/C9DT03883C
45. Oprsal J, Blaha L, Pouzar M, Knotek P, Vlcek M, Hrda K. Assessment of silver nanoparticle toxicity for common carp (Cyprinus carpio) fish embryos using a novel method controlling the agglomeration in the aquatic media. *Environ Sci Pollut Res*. 2015;22(23):19124–19132. doi:10.1007/s11356-015-5120-4
46. Handl J, Malinak D, Capek J, et al. Effects of charged oxime reactivators on the HK-2 cell line in renal toxicity screening. *Chem Res Toxicol*. 2021;34(3):699–703. doi:10.1021/acs.chemrestox.0c00489
47. Čapek J, Hauschke M, Brůčková L, Roušar T. Comparison of glutathione levels measured using optimized monochlorobimane assay with those from ortho-phthalaldehyde assay in intact cells. *J Pharmacol Toxicol Methods*. 2017;88:40–45. doi:10.1016/j.vascn.2017.06.001
48. Majtnerova P, Capek J, Petira F, Handl J, Rousar T. Quantitative spectrofluorometric assay detecting nuclear condensation and fragmentation in intact cells. *Sci Rep*. 2021;11(1):11921. doi:10.1038/s41598-021-91380-3
49. Biola-Clier M, Béal D, Caillat S, et al. Comparison of the DNA damage response in BEAS-2B and A549 cells exposed to titanium dioxide nanoparticles. *Mutagenesis*. 2017;32(1):161–172. doi:10.1093/mutage/gew055
50. Visalli G, Bertuccio MP, Iannazzo D, Piperno A, Pistone A, Di Pietro A. Toxicological assessment of multi-walled carbon nanotubes on A549 human lung epithelial cells. *Toxicol In Vitro*. 2015;29(2):352–362.
51. Jiménez-Chávez A, Solorio-Rodríguez A, Escamilla-Rivera V, et al. Inflammatory response in human alveolar epithelial cells after TiO2 NPs or ZnO NPs exposure: inhibition of surfactant protein A expression as an indicator for loss of lung function. *Environ Toxicol Pharmacol*. 2021;86:103654. doi:10.1016/j.etap.2021.103654
52. Jayaram DT, Payne CK. Intracellular generation of superoxide by TiO2 nanoparticles decreases histone deacetylase 9 (HDAC9), an epigenetic modifier. *Bioconjug Chem*. 2020;31(5):1354–1361. doi:10.1021/acs.bioconjchem.0c00091
53. Runa S, Lakadamyali M, Kemp ML, Payne CK. TiO2 nanoparticle-induced oxidation of the plasma membrane: importance of the protein Corona. *J Phys Chem B*. 2017;121(37):8619–8625. doi:10.1021/acs.jpcb.7b04208
54. Ursini CL, Cavallo D, Fresegna AM, et al. Evaluation of cytotoxic, genotoxic and inflammatory response in human alveolar and bronchial epithelial cells exposed to titanium dioxide nanoparticles. *J Appl Toxicol*. 2014;34(11):1209–1219. doi:10.1002/jat.3038
55. Park E-J, Yi J, Chung K-H, Ryu D-Y, Choi J, Park K. Oxidative stress and apoptosis induced by titanium dioxide nanoparticles in cultured BEAS-2B cells. *Toxicol Lett*. 2008;180(3):222–229. doi:10.1016/j.toxlet.2008.06.869
56. Taurozzi JS, Hackley VA, Wiesner MR. Ultrasonic dispersion of nanoparticles for environmental, health and safety assessment–issues and recommendations. *Nanotoxicology*. 2011;5(4):711–729. doi:10.3109/17435390.2010.528846
57. Ranjan S, Dasgupta N, Sudandiradoss C, Ramalingam C, Kumar A. Titanium dioxide nanoparticle–protein interaction explained by docking approach. *Int J Nanomedicine*. 2018;13:47. doi:10.2147/IJN.S125008
58. Moore TL, Rodriguez-Lorenzo L, Hirsch V, et al. Nanoparticle colloidal stability in cell culture media and impact on cellular interactions. *Chem Soc Rev*. 2015;44(17):6287–6305. doi:10.1039/C4CS00487F
59. Shi H, Magaye R, Castranova V, Zhao J. Titanium dioxide nanoparticles: a review of current toxicological data. *Part Fibre Toxicol*. 2013;10(1):1–33. doi:10.1186/1743-8977-10-15
60. Maier M, Hannebauer B, Holldorff H, Albers P. Does lung surfactant promote disaggregation of nanostructured titanium dioxide? *J Occup Environ Med*. 2006;48:1314–1320. doi:10.1097/01.jom.0000215405.72714.b2
61. Armand L, Biola-Clier M, Bobyk L, et al. Molecular responses of alveolar epithelial A549 cells to chronic exposure to titanium dioxide nanoparticles: a proteomic view. *J Proteomics*. 2016;134:163–173. doi:10.1016/j.jprot.2015.08.006
62. Guadagnini R, Halamoda Kenzaoui B, Walker L, et al. Toxicity screenings of nanomaterials: challenges due to interference with assay processes and components of classic in vitro tests. *Nanotoxicology*. 2015;9(sup1):13–24. doi:10.3109/17435390.2013.829590
63. Bihari P, Vippola M, Schultes S, et al. Optimized dispersion of nanoparticles for biological in vitro and in vivo studies. *Part Fibre Toxicol*. 2008;5(1):1–14. doi:10.1186/1743-8977-5-14
64. Kroll A, Pillukat MH, Hahn D, Schnekenburger J. Interference of engineered nanoparticles with in vitro toxicity assays. *Arch Toxicol*. 2012;86(7):1123–1136. doi:10.1007/s00204-012-0837-z

65. Vrček IV, Pavičić I, Crnković T, et al. Does surface coating of metallic nanoparticles modulate their interference with in vitro assays? *RSC Adv*. 2015;5(87):70787–70807. doi:10.1039/C5RA14100A
66. Ong KJ, MacCormack TJ, Clark RJ, et al. Widespread nanoparticle-assay interference: implications for nanotoxicity testing. *PLoS One*. 2014;9(3):e90650. doi:10.1371/journal.pone.0090650
67. Ahamed M, Akhtar MJ, Alhadlaq HA. Preventive effect of TiO2 nanoparticles on heavy metal Pb-induced toxicity in human lung epithelial (A549) cells. *Toxicol In Vitro*. 2019;57:18–27. doi:10.1016/j.tiv.2019.02.004
68. Ekstrand-Hammarström B, Akfur CM, Andersson PO, Lejon C, Österlund L, Bucht A. Human primary bronchial epithelial cells respond differently to titanium dioxide nanoparticles than the lung epithelial cell lines A549 and BEAS-2B. *Nanotoxicology*. 2012;6(6):623–634. doi:10.3109/17435390.2011.598245
69. Srivastava R, Rahman Q, Kashyap M, et al. Nano-titanium dioxide induces genotoxicity and apoptosis in human lung cancer cell line, A549. *Hum Exp Toxicol*. 2013;32(2):153–166. doi:10.1177/0960327112462725
70. Kansara K, Patel P, Shah D, et al. TiO2 nanoparticles induce DNA double strand breaks and cell cycle arrest in human alveolar cells. *Environ Mol Mutagen*. 2015;56(2):204–217. doi:10.1002/em.21925
71. Wang Y, Cui H, Zhou J, et al. Cytotoxicity, DNA damage, and apoptosis induced by titanium dioxide nanoparticles in human non-small cell lung cancer A549 cells. *Environ Sci Pollut Res*. 2015;22(7):5519–5530. doi:10.1007/s11356-014-3717-7
72. Funahashi S, Okazaki Y, Ito D, et al. Asbestos and multi-walled carbon nanotubes generate distinct oxidative responses in inflammatory cells. *J Clin Biochem Nutr*. 2015;56(2):111–117. doi:10.3164/jcbn.14-92
73. Cavallo D, Fanizza C, Ursini CL, et al. Multi-walled carbon nanotubes induce cytotoxicity and genotoxicity in human lung epithelial cells. *J Appl Toxicol*. 2012;32(6):454–464. doi:10.1002/jat.2711
74. Srivastava RK, Pant AB, Kashyap MP, et al. Multi-walled carbon nanotubes induce oxidative stress and apoptosis in human lung cancer cell line-A549. *Nanotoxicology*. 2011;5(2):195–207. doi:10.3109/17435390.2010.503944